

GPS POSITIONING IMPROVEMENT BY MITIGATING THE IONOSPHERIC HORIZONTAL GRADIENT

NABILA BINTI SA'AT

UNIVERSITI TUN HUSSEIN ONN MALAYSIA

This thesis has been examined on date
and is sufficient in fulfilling the scope and quality for the purpose of awarding the
Degree of Master.

Chairperson:

PROF. MADYA DR. NAFARIZAL NAYAN
Faculty of Electrical and Electronic Engineering
Universiti Tun Hussein Onn Malaysia

Examiners:

PROF. MADYA DR. NORSUZILA BTE YA'COB
Faculty of Electrical Engineering
Universiti Teknologi Mara

DR. MARIYAM JAMILAH BTE HOMAM
Faculty of Electrical and Electronic Engineering
Universiti Tun Hussein Onn Malaysia

GPS POSITIONING IMPROVEMENT BY MITIGATING THE
IONOSPHERIC HORIZONTAL GRADIENT

NABILA BINTI SA'AT

A thesis submitted in
fulfilment of the requirement for the award of the
Degree Master of Electrical Engineering by research

Faculty of Electrical and Electronic Engineering
Universiti Tun Hussein Onn Malaysia

AUGUST 2016

*I dedicate this entire work to my beloved parents, Sa'at & Adidah,
my sisters, Narisa & Nasrin,
my nephew, Naseem,
and all my friends
for their support and encouragement that has
constantly been a part of this journey.*

In the end, it is the journey that matters along with prayer and food!

ACKNOWLEDGEMENT

First, thanks to Allah the All Mighty for giving me health and prosperity to complete this study. Peace be upon Prophet Muhammad S.A.W., may Allah bless him.

A special mention must go to my supervisor, Dr. Karthigesu A/L Nagarajoo, for his encouragements, patience, ideas and guidance throughout the entire project. I must highlight that he has done a good deal more for me than most of any supervisors. Thanks a lot!

Special thanks to those in charge who provided me the data needed in this project and gave valuable technical guidance in this project.

Lastly, I am sincerely grateful to my beloved family especially my parents who had given me their trust, spiritual encouragement and support throughout the duration of the project and not forgetting my friends for their help and always be by my side. I also would like to extend my thanks to everyone whom directly or indirectly, have lent their helping hands in this venture.

ABSTRACT

A 3D ionospheric model was developed using TC3D and IRI to enhance the effect of the ionosphere to the GPS signals. Four comparisons have been done to see the effect of the DGPS positioning such as baselines length (short and long), low and high solar activity, range measurement from three and eight satellites and two different duration times (one and three hours). Some improvements can be seen after the corrections and it was a noticeable positioning improvement at the user location over the equatorial region. Improvement in the final positioning error can be found for all cases; with and without ionospheric corrections. From the results, positioning improvement has been achieved where only 26% of percentage error is from short baseline, 27% of percentage error from low solar activity, percentage error from 24% of 8 satellites and 40% of 3 hours period of time. It shows that it is important to consider criteria such as shorter baseline with more satellites viewing for longer duration of time (in hour) during low solar activity to achieve the improvement in the positioning. The effect of the ionospheric horizontal gradient which is more noticeable in the equatorial region has been resolved and will be very beneficial to improve the positioning of the user location, especially in applications such as surveying, geophysics, navigation and aviation.

ABSTRAK

Model 3D ionosfera telah dibangunkan dengan menggunakan TC3D dan IRI bagi meningkatkan kesan ionosfera ke atas isyarat GPS. Empat perbandingan telah dilaksanakan bagi melihat kesan daripada kedudukan DGPS seperti ukuran garis dasar (pendek dan panjang), aktiviti solar tinggi dan rendah, pengukuran daripada tiga dan lapan buah satelit dan dua tempoh masa yang berbeza (satu dan tiga jam). Beberapa penambahbaikan dapat dilihat selepas pembetulan tersebut dan ini merupakan peningkatan ketara kedudukan di lokasi pengguna rantau Khatulistiwa. Peningkatan dalam ralat kedudukan terakhir boleh didapati untuk semua kes; dengan dan tanpa pembetulan ionosfera. Daripada keputusan, kedudukan peningkatan yang telah dicapai di mana hanya 26% daripada ralat peratusan dari garis dasar pendek, 27% daripada ralat peratusan daripada aktiviti solar rendah, ralat peratusan daripada 24% daripada 8 satelit dan 40% daripada tempoh masa 3 jam telah ditunjukkan. Ia menunjukkan adalah penting untuk mempertimbangkan kriteria seperti garis dasar yang lebih pendek dengan lebih satelit bagi jangka masa yang lebih lama (dalam jam) semasa aktiviti solar rendah bagi mencapai peningkatan dalam penentududukan. Kesan kecerunan mendatar ionosfera yang lebih ketara di kawasan khatulistiwa dapat diselesaikan dan akan menjadi sangat bermanfaat untuk meningkatkan kedudukan lokasi pengguna, terutamanya dalam aplikasi seperti pengukuran, geofizik, navigasi dan penerbangan.

CONTENTS

TITLE	i
DECLARATION	ii
DEDICATION	iii
ACKNOWLEDGMENT	iv
ABSTRACT	v
CONTENTS	vii
LIST OF TABLES	x
LIST OF FIGURES	xi
LIST OF ABBREVIATIONS	xiii
LIST OF APPENDICES	xv
CHAPTER 1 INTRODUCTION	1
1.1 Project background	1
1.2 Problem statement	2
1.3 Research objectives	3
1.4 Scope of the project	3
1.5 Thesis outline	3
CHAPTER 2 LITERATURE REVIEW	5
2.1 Introduction to Ionosphere	5
2.2 Structures of Ionosphere	5

2.2.1	D region (60 to 90 km)	7
2.2.2	E region (100 to 125 km)	7
2.2.3	F region (140 to 500 km)	8
2.3	Variation in the Ionosphere	8
2.4	Total Electron Content (TEC)	9
2.5	Global Positioning System (GPS)	10
2.6	GPS signals	11
2.7	Differential GPS (DGPS)	12
2.8	Horizontal Gradient	13
2.9	Positional Dilution of Position (PDOP)	14
2.10	Solar Activity	16
2.11	Geomagnetic K_p and A_p Indices	17
CHAPTER 3 METHODOLOGY		19
3.1	Introduction	19
3.2	International Reference Ionosphere (IRI)	21
3.3	Table Curve 3D (TC3D)	22
3.4	Trimble Business Center (TBC)	25
CHAPTER 4 RESULTS AND ANALYSIS		32
4.1	Introduction	32
4.2	Validation of the Electron Density Model from IRI and TC3D using Matlab	32
4.3	Modelling the Diurnal Variation of Ionosphere in Longitude and Latitude over the Equatorial Region	36
4.4	Effect of Equatorial Ionospheric Horizontal Gradient to DGPS positioning	42
4.4.1	DGPS Positioning Improvement between short baseline and long baseline	42

4.4.2	DGPS Positioning Improvement during low solar activity (2009) and high solar activity (2012)	44
4.4.3	DGPS Positioning Improvement by using 3 and 8 satellites	46
4.4.4	DGPS Positioning Improvement for different duration of times	49
4.5	Summary	51
CHAPTER 5	CONCLUSION AND RECOMMENDATIONS	53
5.1	Conclusions	53
5.2	Recommendations	54
	REFERENCES	55
	LIST OF PUBLICATIONS	61
	APPENDIX	62
	VITA	69

LIST OF TABLES

2.1	DOP ratings	15
2.2	Equivalent range A_p for given K_p	18
4.1	The comparison value of N_e from IRI, TC3D and Matlab	36
4.2	The comparison of the distance after ionospheric correction for NTUS-UKM data (long distance)	42
4.3	The comparison of the distance after ionospheric correction for NTUS – ISK data (short distance)	43
4.4	Positioning improvement for NTUS – UKM (long distance) data	43
4.5	Positioning improvement for NTUS – ISK (short distance) data	44
4.6	Ionospheric correction data from low solar activity (2009) data	45
4.7	Ionospheric correction data from high solar activity (2012) data	45
4.8	Positioning improvement for low solar activity (2009) data	45
4.9	Positioning improvement for high solar activity (2012) data	46
4.10	The comparison of three satellites after correction for NTUS – ISK data	47
4.11	The comparison of eight satellites after correction for NTUS – ISK data	47
4.12	Positioning improvement for three satellites data	48
4.13	Positioning improvement for eight satellites data	48
4.14	The comparison of 12.00 pm to 1.00 pm (one hour) after correction for NTUS – ISK data	49
4.15	The comparison of 12.00 pm to 3.00 pm (three hours) after correction for NTUS – ISK data	49
4.16	Positioning improvement at 12.00 pm to 1.00 pm	50
4.17	Positioning improvement at 12.00 pm to 3.00 pm	50

LIST OF FIGURES

2.1	Earth's atmospheric layer	6
2.2	View of the layers in the ionosphere over the period of a day	7
2.3	The segment of GPS	11
2.4	Differential GPS concept	13
2.5	Illustration of good and bad geometric dilution of precision	15
2.6	Cycle 24 sunspot number predictions	16
3.1	Flow chart for overall project	20
3.2	Part of the cross section of IRI-2012	22
3.3	Table Curve 3D automated fitting process	23
3.4	The equation list after surface fit all equations	24
3.5	Flow chart of modelling the diurnal variation of ionosphere over equatorial region	25
3.6	Plan view displays in TBC window	27
3.7	Flow chart of the effect of equatorial ionospheric horizontal gradient to DGPS positioning	31
4.1	The fitted values (from equation 539) and the values of the N_e from IRI at latitude from 0 to 50° for the region of longitude from 100 to 120°	34
4.2	The fitted values (from equation 539) and the values of the N_e from IRI at longitude from 100 to 120° and for the region of latitude from 0 to 50°	34
4.3	The contour plot of N_e on 1 st June 2009 at 4 different times	37
4.4	The contour plot of N_e on 2 nd June 2009 at 4 different times	38
4.5	The contour plot of N_e on 3 rd June 2009 at 4 different times	38
4.6	The contour plot of N_e on 4 th June 2009 at 4 different times	40
4.7	The contour plot of N_e on 5 th June 2009 at 4 different times	40
4.8	The contour plot of N_e on 6 th June 2009 at 4 different times	41

4.9	The contour plot of N_e on 7 th June 2009 at 4 different times	41
4.10	The percentage error	52

LIST OF ABBREVIATIONS

CORS	Continuously Operating Reference Station
COSPAR	Committee on Space Research
CS	Control Segment
DGPS	Differential Global Positioning System
EUV	Extreme Ultraviolet
GNSS	Global Navigation Satellite System
GPS	Global Positioning System
HF	High Frequency
IRI	International Reference Ionosphere
ISK	IskandarNet Station
K_p	Geomagnetic K-index
L_1	Prime GPS Carrier Frequency (1557.42 MHz)
L_2	Secondary GPS Carrier Frequency (1227.6 MHz)
LF	Low Frequency
LT	Local Time
MEO	Medium Earth Orbit
MF	Medium Frequency
NASA	National Aeronautics and Space Administration
N_e	Electron Density
NGS	National Geodetic Survey
NOAA	National Oceanic and Atmospheric Administration
NTUS	Nanyang Technological University Singapore
PDOP	Positioning Dilution Of Precision
RMS	Root Mean Square
SPS	Standard Positioning Service
SS	Space Segment
SSE	Sum of Squared Error

sTEC	Slant Total Electron Content
SV	Space Vehicles
TBC	Trimble Business Center
TC3D	Table Curve 3 Dimension
TEC	Total Electron Content
TECU	Total Electron Content Unit
URSI	International Union of Radio Science
UV	Ultraviolet
VHF	Very High Frequency
VLF	Very Low Frequency
WOC	without correction

LIST OF APPENDICES

APPENDIX	TITLE	PAGE
A	Sample of Data Summary from TC3D	62
B	Sample of Numeric Summary from TC3D	63
C	Sample of Observation Data	67

CHAPTER 1

INTRODUCTION

1.1 Project background

Ionosphere is one of the atmospheric layers that play an important role in radio communication. The ionospheric layer is formed by free electrons or sometimes termed as electron density concentration varies with height or distance from the Earth's surface, latitude, time of day, season, and amount of solar activity [1]. For high frequency (HF) propagation (3 to 30MHz), ionospheric layer acts as a conductive region which reflects the radio wave signals at specific frequencies to any radio receiver station on the Earth. However, for transionospheric propagation, it acts as a dispersive medium for some radio signals (in the range of 30MHz to 3GHz). Those radio signals' speed of propagation or termed as group path will be delayed.

Ionosphere is prone to significant disturbances, which get considerably worst during periods of high solar activity [2]. Due to that, and as was mentioned above, the radio signals that propagates through the ionosphere suffers increment of group path delay which is proportional to the content of free electrons. The scenario is worst for the radio signals that propagate over the equatorial region. The fact that the ionosphere is formed by the radiation from the Sun suggests that this mechanism results in variations in the ionosphere with time of day, season, solar cycle and position on the Earth surface. The travel time of Global Positioning System, (GPS) satellite signals can be altered by atmospheric effects; when a GPS signal passes through the ionosphere it is refracted, causing the speed of the signal to be different

from the speed of a GPS signal in space. Sunspot activity also causes interference with GPS signals [3].

The GPS signals will be delayed as they propagate through the ionosphere. The ionosphere will introduce a significant amount of added group delay which will affect the final GPS positioning, if the ionospheric error is not corrected. An example of large ionosphere gradients that could cause the significant GPS user errors have been observed [4]. A number of studies have been done and is still continuing to mitigate the ionospheric horizontal gradient by using variety of methods in order to improve the final user positioning [5]–[8]. For any GPS applications over the equatorial region (i.e. navigation, surveying, mapping, mining, agriculture and automatic aircraft landing), the ionospheric error and the horizontal gradient effect need to be corrected in order to determine the most accurate or precise GPS final positioning. Many researches also have investigated the GPS positioning improvement using different methods for different range of conditions [9]–[11].

In this research, first of all, the effect of the ionosphere over the equatorial region (e.g. Malaysia) has been investigated. Then, three dimensional analytical mathematical models have been developed to represent the actual formation of the ionosphere over the equatorial region. The existing ionospheric online-database such as International Reference Ionosphere (IRI) [12], which contains the value of electron density at various location and time, was used to do the analytical modeling. After that, the characteristics of the GPS signals as they propagate through the ionosphere have been determined. By doing so, the effect of the ionosphere to GPS positioning has been obtained. To further the research work, GPS positioning improvement were done by mitigating the ionosphere horizontal gradient using Trimble Business Center (TBC) software.

1.2 Problem statement

Over the equatorial region, the formation of the ionosphere introduces greater ionospheric horizontal gradient which could give greater positioning error for a user station in a GPS system. The ionospheric horizontal gradient is the variation of electron density with latitude and longitude which can cause the azimuthally deviation of the GPS ray path. The electron density in the ionosphere will cause

greater refraction to the GPS signals as it propagates through it. Due to the refraction, the final GPS positioning is not accurate. GPS positioning accuracies are affected by different error sources. Therefore, TBC software will be used in order to mitigate the effect of the ionosphere to GPS signals and a 3 dimensional (3D) analytical mathematical model will be developed using IRI.

1.3 Research objectives

The objectives of this research:

1. To determine the ionospheric effect over the equatorial region.
2. To develop the 3D analytical mathematical model.
3. To analyze and mitigate the ionosphere horizontal gradient using TBC software for positioning.

1.4 Scope of the project

1. The region of this study is focused only from the middle to the southern region of Peninsular Malaysia
2. Data was taken from stations of Nanyang Technology University Singapore (NTUS) (1.34°N, 103.7°E), Universiti Kebangsaan Malaysia (UKM) (9.92°N, 101.7°E) and ISKANDARnet (ISK) (1.56°N, 103.6°E) on June 2009 (low solar activity) and August 2012 (high solar activity).

1.5 Thesis outline

In general, this thesis consists of five chapters. Each chapter will discuss on different issues related to the project.

The first chapter describes an overview of the project background, problem statement, research objectives and scope of the study to carry out the project.

Chapter two focuses on the review from previous studies that was made which was helpful to gain knowledge and to understand the project better. It presents some general review of the ionosphere and basic principles on GPS and its characteristic.

Chapter three elaborates the methodology of the research. This project requires a lot of simulations such as using IRI to obtain electron density, Table Curve 3D (TC3D) for calculation and viewing the 3D graph, and TBC software to improve GPS positioning.

Chapter four contains the details of data that was analyzed. It also contains the discussion from this research. Comparisons are made to determine the best result.

Lastly, chapter five includes the conclusions and recommendations that can be done in the future related to this study.

CHAPTER 2

LITERATURE REVIEW

2.1 Introduction to Ionosphere

The Earth's atmosphere is a thin layer of gases that surrounds the Earth. It is composed of 78% of nitrogen, 21% of oxygen and 1% of other gases such as argon and carbon dioxide [13]. This thin gaseous layer insulates the Earth from extreme temperatures; keeps heat inside the atmosphere and also blocks the Earth from the Sun's incoming ultraviolet radiation. The ionosphere, which is found from the altitude of about 60km to 700km, contains up to four layers of free electrons which can enable long-distance radio communication [14]. The GPS signals that are propagated through the atmosphere are affected by several conditions such as variation at different altitudes (height from the surface of Earth), geographical location, diurnal and seasonal changes, and also due to the changes in the Sun's solar activity. The Earth's atmosphere consists of a few layers as can be seen in Figure 2.1.

Ionosphere was formed when extreme ultraviolet (EUV) light from the Sun strips the electrons from the neutral atoms of the Earth atmosphere [15]. This neutral atom known as positive ion when it has lost negative charged electron. This process is known as photoionization [15]. In contrast, recombination is the reverse of photoionization [15]. The rate at which ionization occurs depends on the density of atoms in the atmosphere and the intensity of the EUV, which varies with the activity of the Sun [16].

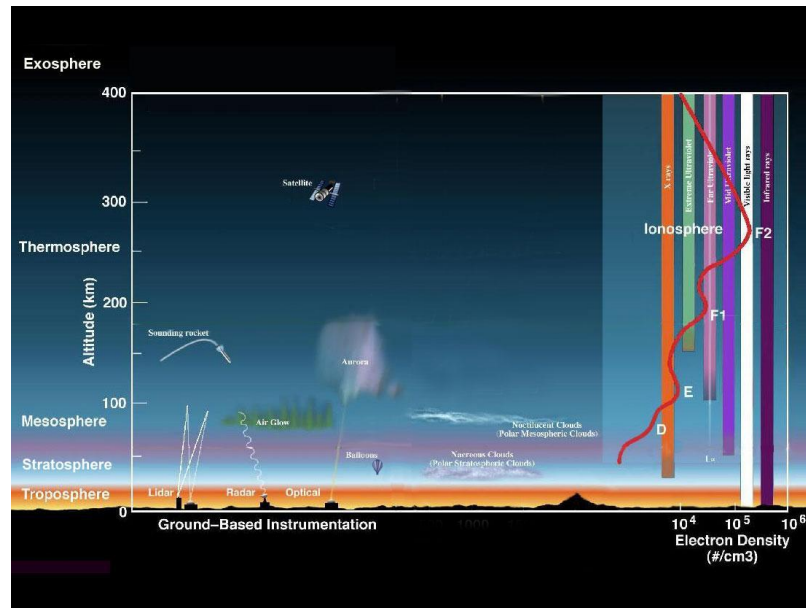


Figure 2.1: Earth's atmospheric layer [17]

During late afternoon and early evening hours, the rate of recombination exceeds the rate of ionization. Due to this, the density of the ionized layers normally begins to decrease in the D, E and F₁ layers at this time. However, the F₂ layer acts differently. The electron density in the F₂ layer reaches its lowest value just before dawn [18]. Then, once the Sun rises, photoionization takes place which causing the content of electron density to increase again in the F₂ layer. That is the reason for the ionosphere can still be used at night time for HF or ionospheric reflected radio wave propagation. Other than recombination, the protonosphere also plays a role here. The protonosphere acts like a reservoir as there is no plasma production in the protonosphere [19]. It takes plasma from the ionosphere by day, stores it in a loss-free environment and returns it to the ionosphere at night, which helps to maintain the F layer during night time.

2.2 Structures of Ionosphere

The ionosphere is composed of D, E and F layers, named in the order of increasing height as in Figure 2.2. During day time, the radiation of the sun is high on the local atmosphere. At this time, all the layers will exist. At night time or when there is no radiation, the ions and electrons will recombine (recombination process). Only the F₂ layer will be seen since the other three layers (D, E and F₁) almost completely

disappear due to the recombination process. The ionosphere is composed of the D, E, F₁ and F₂ regions, named in order of increasing height.

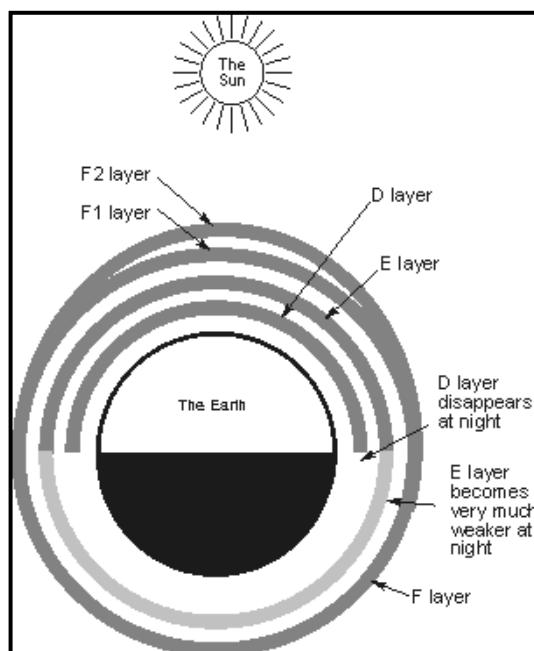


Figure 2.2: View of the layers in the ionosphere over the period of a day [20]

2.2.1 D region (60 to 90 km)

The D region is the bottom layer of the ionosphere that affects radio communication signals to any degree. It is only present during the day to an extent that affects radio waves noticeably. It mainly has absorbing or attenuating radio communication signals particularly in the LF and MF portions of the radio spectrum, reducing with frequency. At night it has little effect on most radio communication signals although there is still a sufficient level of ionisation for it to refract VLF signals.

2.2.2 E region (100 to 125 km)

Instead of attenuating radio communication signals this layer chiefly refracts them, often to a degree where they are returned to Earth. As such they appear to have been reflected by this layer. However this layer still acts as an attenuator to a certain degree. Like the D region, the level of ionisation falls relatively quickly after dark as

the electrons and ions re-combine and it virtually disappears at night. However the residual night time ionisation in the lower part of the E region causes some attenuation of signals in the lower portions of the HF part of the radio communications spectrum.

2.2.3 F region (140 to 500 km)

This is the most important layer of the ionosphere for HF and transionospheric radio wave propagation. It exists from an altitude of about 140 km to 400km and sometimes up to 500 km. During daytime, the F layer will split into two layers; termed as the F_1 and F_2 layers. The F_1 layer is in the altitude range from 130 to 210 km whereas the F_2 layer is from 210 to 400 km; sometimes up to 500 km. It also has been found that, at mid latitudes, the F_2 layer has a higher electron concentration during day time in winter than in summer. This unexpected behaviour in the F_2 layer is called the mid-latitudes seasonal anomaly. Due to their larger electron density, the F_2 layer, and to some extent the F_1 layer, are the major source of ionospheric induced error for range finding and positioning at GPS frequencies.

2.3 Variation in the Ionosphere

The regular variations in ionosphere often known as daily, seasonal, geographical location, latitude and solar cycle variations. The frequencies available for HF communications and other uses of the ionosphere have the same variations and it is important to the propagation of radio waves. For 24-hour diurnal (night/day) variation, rotation of the Earth on its axis, producing daily ionospheric changes [21]. In seasonal variation, the Earth revolving around the sun; the relative position of the Sun moves from one hemisphere to the other with changes in seasons [21]. Latitudinal variation cause by the variation with solar zenith angle and the curvature of Earth causes a geographical variation in the ionospheric electron concentration [22]. Regular solar cycle variation of sunspot activity has a minimum and maximum level and occurs approximately every 11 years [21] and thus produce solar cycle variation.

2.4 Total Electron Content (TEC)

Total Electron Content (TEC) is an important descriptive quantity for the ionosphere. TEC is the total number of electrons present along a path between two points, with units of electrons per square meter, where 1×10^{16} electrons/m² = 1 TEC unit (TECU) [23]. The ionospheric TEC predictions using dual frequency technique and TEC map using Bernese GPS software (BGS) with PPP technique showed that TEC have similar variations, where the TEC values start to increase gradually from morning and reach its maximum in the early afternoon and decrease just before sunrise [24]. TEC during the day was higher than at night and during the low solar activity. It varies from a pre-dawn minimum to a maximum during the afternoon and then decreases [25]. The low values of TEC are observed in winter and high values observed in equinox [26].

TEC is one of the most important parameters that describe the ionospheric state and structure. Theoretically, different periods of ionospheric physical process can be studied by detecting and analyzing the temporal variations of TEC. TEC can be used to correct the radio wave propagation in the space-based radio communication application like satellite position, navigation and orbit determination, because TEC is closely associated with the time delay of the radio wave.

Computing TEC from GPS data is feasible due to the dispersive nature of the ionosphere, which affects the speed of propagation of the electromagnetic waves transmitted by the GPS satellites on two L-band frequencies ($L_1=1575.42$ MHz and $L_2=1227.60$ MHz) as they travel through that region of the atmosphere. The change in satellite-to-receiver signal propagation time due to the ionosphere is directly proportional to the integrated free-electron density along the signal path. GPS pseudorange measurements are increased (the signal is delayed) and the carrier-phase measurements are reduced (the phase is advanced) by the presence of the ionosphere. After forming the linear combination of these measurements on the L_1 and L_2 frequencies, the carrier phase and the pseudorange TEC are obtained.

Slant TEC (*sTEC*) is a measure of the total electron content of the ionosphere along the ray path from the satellite to the receiver. It can be calculated by using pseudorange measurements as in equation (2.1) below:

$$sTEC = \frac{1}{40.3} \left(\frac{f_1^2 f_2^2}{f_1^2 - f_2^2} \right) (P_2 - P_1) \quad (2.1)$$

Where;

$f_1 = 1575.42$ MHz (high GPS frequency)

$f_2 = 1227.6$ MHz (low GPS frequency)

P_1 and P_2 are the pseudoranges measured (in distance unit) in L_1 and L_2 , respectively

The fundamental navigation principle is based on the measurement of pseudoranges between the user and four satellites. Ground stations precisely monitor the orbit of every satellite and by measuring the travel time of the signals transmitted from the distance of four satellites between receiver and satellites will yield accurate position, direction and speed. The term of ‘pseudoranges’ is obtained when the fourth observation is essential for solving clock synchronization error between receiver and satellite though three-range measurements are sufficient [27].

2.5 Global Positioning System (GPS)

Global navigation satellite system (GNSS) is a generic reference for any navigation system based on satellites; the system in widespread use today is the United States' global positioning system (GPS) [28]. GPS is now widely available for use by many applications. GPS consists of three segments: the space segment, the control segment, and the user segment [29] as shown in Figure 2.3. Twenty-four satellites (the space segment) in orbit around the Earth send data via radio links that allows aircraft receivers (the user segment) to calculate precise position, altitude, time and speed on a 24-hour, worldwide, all weather basis. The principles of satellite navigation are based on radio wave propagation, precision timing and knowledge of each satellite's position above the Earth; this is all monitored and controlled by a network of stations (the control segment) [28].

The main purpose of the GPS is to determine the position and velocity of a fixed or mobile object, placed over or near the Earth surface, using the signals of the satellites. A GPS receiver calculates its position by precisely timing the radio signals sent by the GPS satellites high above the Earth. The receiver measures the transit time of each message and computes the distance to each satellite [30]. Study showed that the seasonal variation is a major factor for determining the accuracy of GPS

measurements and also, increasing the observation period hardly improves the horizontal positioning accuracy while improving the vertical positioning accuracy [11]. It seems 3 satellites are enough to solve for position, since it is 3 dimensions at space (latitude, longitude, altitude). However, study shows the range measurements from more satellites (for example 8 satellites) can give better positioning [31].

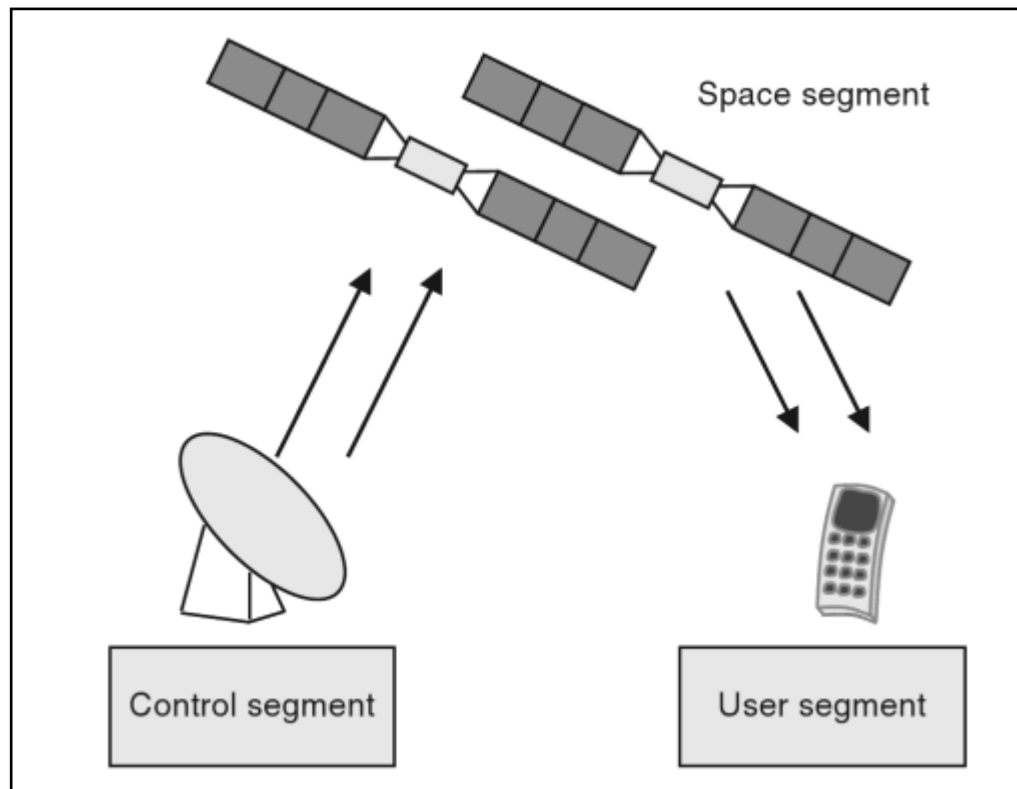


Figure 2.3: The segment of GPS [32]

2.6 GPS signals

Each GPS satellite transmits microwave radio signal which are two carrier frequencies (or sine wave) modulated by two digital codes and navigation message [33]. The availability of the two carrier frequencies allows for correcting major GPS errors, known as the ionospheric delay.

The two GPS codes are called coarse acquisition (or C/A-code) and precision (or P-code). Each code consists of a stream of binary digits, zeros and ones, known as bits or chips. The codes are commonly known as PRN codes because they look

like random signals. But in reality the codes are generated using mathematical algorithms.

2.7 Differential GPS (DGPS)

Differential GPS (DGPS) is a technique for reducing the error in GPS derived positions by using additional data from the reference GPS receiver at a known position. DGPS developed by the U.S Coast Guard to augment Standard Positioning Service (SPS) [29]. DGPS was used by many civilian GPS receivers to greatly improve accuracy.

DGPS involves the cooperation of two receivers, making position measurements. For the standard DGPS method, GPS measurement at two spaced receiving stations; one of which is at reference station, where the effect of the ionosphere can be determined and used to correct the range measurement at the mobile station [10]. The most common form of DGPS involves in determining the combined effect of navigation message ephemeris and satellite clock errors at a reference station and transmitting pseudorange corrections, in real time, to a user's receiver, which applies the correction in the process of determining its position [34]. This reference station receives the same GPS signals as the mobile station but instead of working like a normal GPS receiver it attacks the equations backwards. Instead of using timing signals to calculate its position, it uses its known position to calculate timing. The receiver then transmits this error information to the mobile receiver station so it can use it to correct its measurements [35]. The positioning of a mobile station in real time by corrected GPS pseudo-ranges. The corrections are determined at a static "reference station" and transmitted to the mobile station. A monitor station may be part of the system, as a quality check on the reference station transmissions. The differential GPS concept is shown in Figure 2.4. A positioning accuracy of 1 to 5 m can be provided by DGPS depending on the mobile reference separation and, to a lesser extent on the mobile platform dynamics and the processing complexity. Research in [36] proposed a method in reducing the positioning error caused by the length of baseline in getting precise positioning by DGPS.

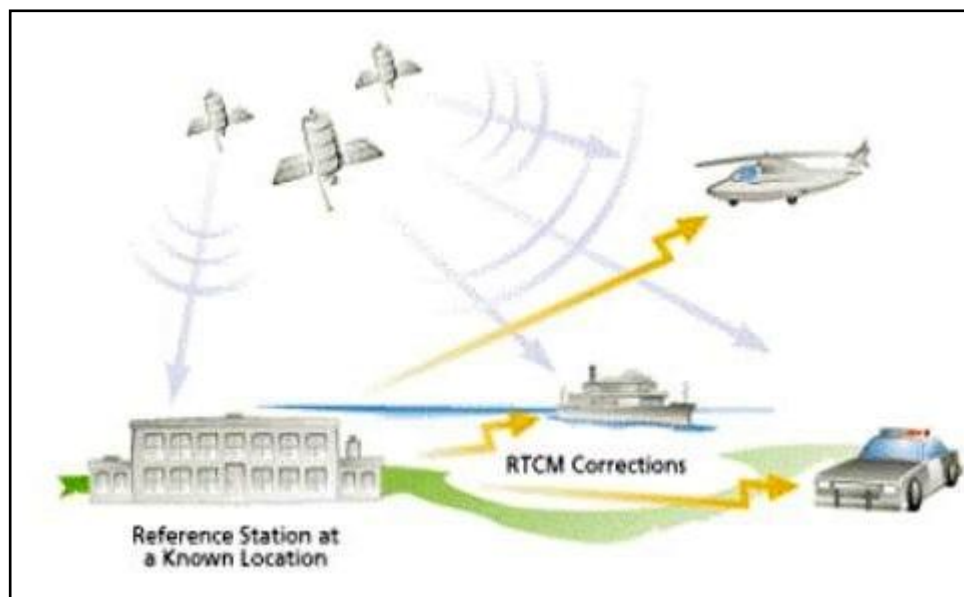


Figure 2.4: Differential GPS concept [37]

2.8 Horizontal Gradient

DGPS is a system where the range error at a reference station will be eliminated from the range measurement at the user station, which ‘view’ the same satellite, presuming that the satellite’s path to both the reference station and the user experience common errors due to the ionosphere, clock errors, multipath and etc. In this assumption, the error due to the ionospheric refraction is assumed to be the same for the two closely spaced paths and thus the presence of ionospheric horizontal gradient is ignored. If a user’s path is exposed to a drastically large ionosphere gradient (i.e. over the equatorial region), the large difference of ionosphere delays between the reference and the user stations can result in significant position error at the user station.

The ionospheric horizontal gradient has greater effect for the DGPS user position over the equatorial region [6]. However, after the mitigation process, the error could be reduced. There is method to obtain the magnitude and direction of the gradient from real data. In [38] the dual frequency method has been used to obtain both South-North and East-West gradients by using four different receiving stations separated in those directions. It can be estimated from the gradient in $sTEC$ observed from the received GPS satellites or based on an empirical model updated with real-time data, or both.

The effect of an ionospheric horizontal gradient that cause an error in DGPS positioning has been investigated to obtain a more accurate ionospheric correction for DGPS [39]. By performing ray-tracing calculations with and without a linear horizontal ionosphere gradient, the effects of ionospheric horizontal gradient have been separated and a final positioning improvement has been shown at the user of a DGPS system over the equatorial region.

In the context of Local Area Augmentation System (LAAS), [4] study the presence of stationary ionospheric gradients and their effect on the GPS Signals. Large ionosphere gradients that could cause the significant user errors have been observed at low/equatorial latitudes even within a distance of approximately 4km a maximum gradient of 460mm/km, which is comparatively very high. Hence, there is necessity to enhance upper bound for the ionospheric gradients threat space over low latitudes.

2.9 Positional Dilution of Position (PDOP)

Positional Dilution of Position (PDOP) refers to the geometric positioning of the satellites that are being used to calculate a position (measure of accuracy in 3-D position). An ideal geometric positioning of satellites is one in which four or more satellites are distributed evenly throughout the sky [40]. A poor geometry is one in which satellites are clustered together in the sky, with many satellites directly overhead or nearly so. As the satellite geometry shift away from the ideal situation, PDOP increases [40].

PDOP is a unitless value that expresses the relationship between the error in user and the satellite position. It describes how well or bad the satellites' geometry for a user and indicates when the satellite geometry can provide the most accurate results.

Table 2.1: DOP ratings [41]

DOP Value	Ratings
1	Ideal
2-4	Excellent
4-6	Good
6-8	Moderate
8-20	Fair
20-50	Poor

A low DOP indicates a higher probability of accuracy as shown in Table 2.1. A high DOP indicates a lower probability of accuracy. The quality of the data decreases as the PDOP value increases [41]. Due to the presence of ionospheric disturbances, satellite geometry was also affected. Study in [42] showed that in a disturbed ionosphere the maximum value of PDOP varied between 3 and 4 which is high compared to quiet ionospheric conditions which varied between 0.8 and 1.5.

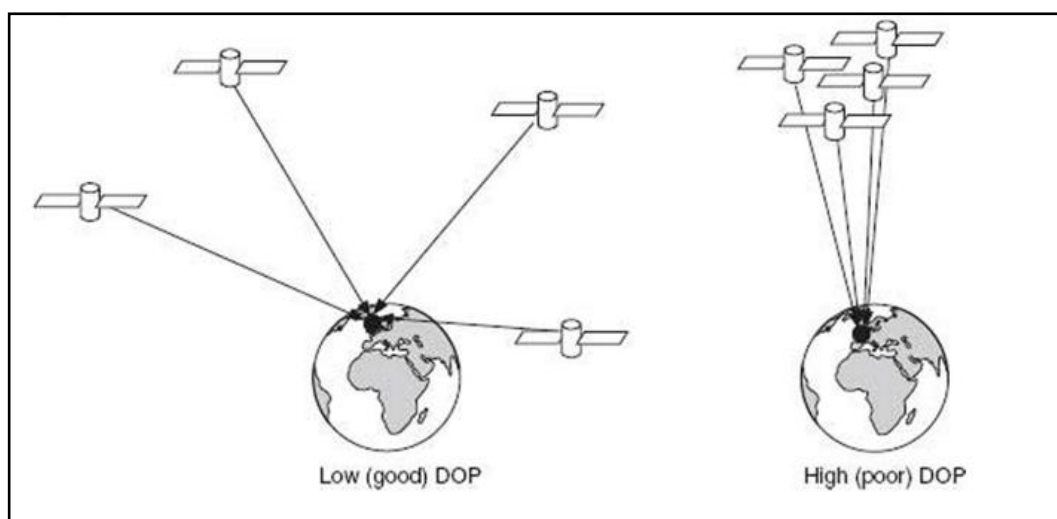


Figure 2.5: Illustration of good and bad geometric dilution of precision [43]

The concept of the geometric dilution of precision is more clearly illustrated in Figure 2.5. When the visible satellites are widely spread in the sky, pseudorange error is minimized; however, when visible satellites are closely spaced, the uncertainty is increased [43].

2.10 Solar Activity

In general, the electron density in the ionosphere is greatest during summer, in the middle of day, and near the equator. The radiation of the Sun heats the air near the surface, most strongly in equatorial regions where the Sun is directly overhead [44]. The accuracy of the GPS positioning in summer is higher than in winter was shown in [11]. The ionosphere also varies with significantly with solar activity, the amount of EUV radiation from the sun waxes and wanes every 11 years. The UV radiation from the Sun is influenced by the number of sunspots on the Sun's "surface", which shows a cycle of about 11 years (see Figure 2.6).

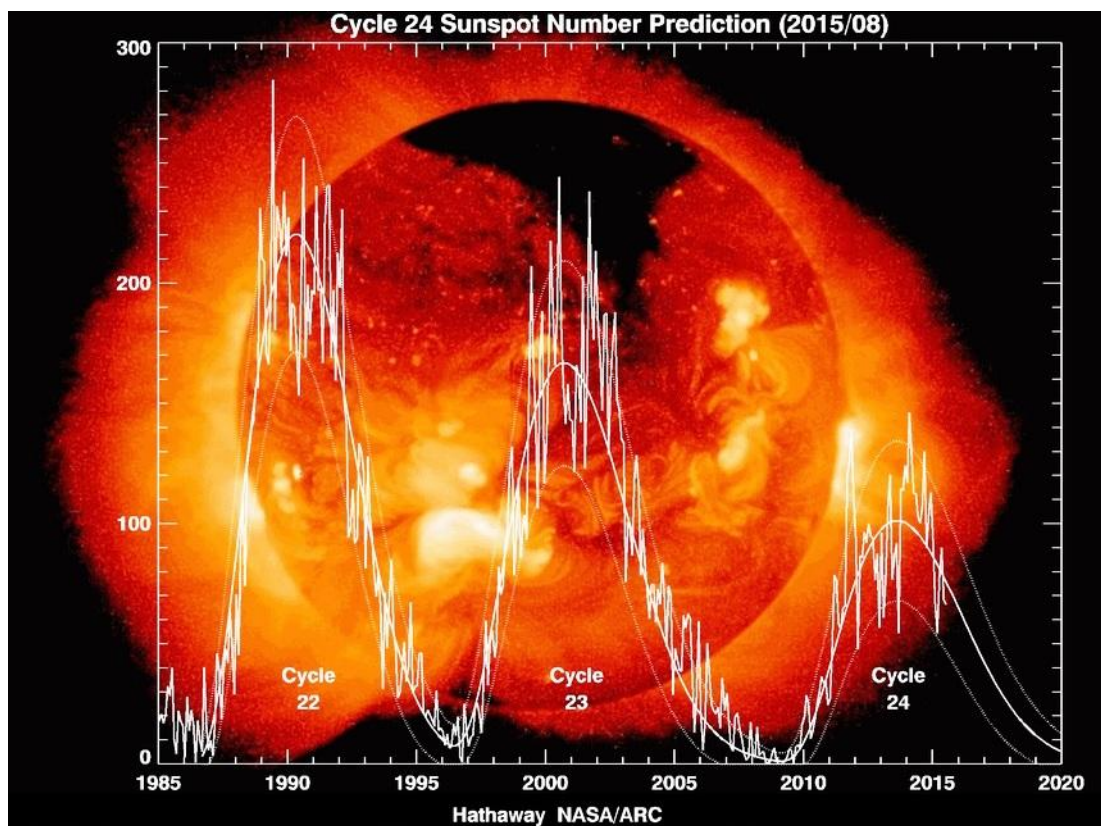


Figure 2.6: Cycle 24 sunspot number predictions [45]

The sunspot number clearly goes up and down every 11 years; it has a cycle of about 11 years. Virtually everything associated with the Sun of relevance to the ionosphere occurs with an approximately 11 year cycle, hence the name solar cycle. The previous solar cycle (Cycle 23) starts in about 1998 and ends in 2009. That is why 2009 has the lowest solar cycle as very few, and only relatively small,

sunspot-carrying active regions were observed [46]. In current solar cycle, which is solar cycle 24, the solar activity is maximum. According to NOAA and NASA, the sunspot cycle hit an unusually deep bottom from 2007 to 2009. In fact, in 2008 and 2009, there were almost no sunspots, a very unusual situation that had not happened for almost a century [47]. The Sun is getting more active with resulting in ionospheric disturbances at high latitudes and in equatorial regions. One effect is increased ionospheric delays [3]. The sunspot number is used as a parameter to compare the values of critical frequency at high and low sunspot numbers for the day. Although sunspots themselves produce only minor effects on solar emissions, the magnetic activity that accompanies the sunspots can produce dramatic changes in the ultraviolet and soft x-ray emission levels [48]. Solar variation causes changes in space weather and climate and has important consequences for the Earth's upper atmosphere. It causes a periodic change in the amount of irradiation from the Sun that is experienced on the Earth. The years of high solar activities correspond to high electron density, while the years of low solar activities are also years of low electron density [49].

2.11 Geomagnetic K_p and A_p Indices

Daily regular magnetic field variation arises from current systems caused by regular solar radiation changes. Other irregular current systems produce magnetic field changes caused by the interaction of the solar wind with the magnetosphere; by the magnetosphere, by the interactions between the magnetosphere and ionosphere, and by the ionosphere itself [50]. Magnetic activity indices were designed to describe variation in the geomagnetic field caused by these irregular current systems.

K indices isolate solar particle effects on the Earth's magnetic field; over a three-hour period, they classify into disturbance levels the range of variation of the more unsettled horizontal field component. Each activity level relates almost logarithmically to its corresponding disturbance amplitude. Three-hour indices discriminate conservatively between true magnetic field perturbations and the quiet-day variations produced by the ionospheric currents.

K indices range in 28 steps from 0 (quiet) to 9 (greatly disturbed) with fractional parts expressed in thirds of a unit. A K -value equal to 27, for example,

means 2 and 2/3 or 3-; a K -value equal to 30 means 3 and 0/3 or 3 exactly; and a K -value equal to 33 means 3 and 1/3 or 3+. This planetary index is designed to measure solar particle radiation by its magnetic effects [51]. During an ionospheric disturbed day, K_p index showed a value greater than 4, while during quiet day, the K_p index value remained below 2 [42].

Table 2.2: Equivalent range A_p for given K_p [50]

K_p	0o	0+	1-	1o	1+	2-	2o	2+	3-	3o	3+	4-	4o	4+
A_p	0	2	3	4	5	6	7	9	12	15	18	22	27	32
K_p	5-	5o	5+	6-	6o	6+	7-	7o	7+	8-	8o	8+	9-	9o
A_p	39	48	56	67	80	94	111	132	154	179	207	236	300	400

Table 2.2 shows the A -index ranges from 0 to 400 and represents a K -value converted to a linear scale in gammas (nanoTeslas), a scale that measures equivalent disturbance amplitude of a station at which $K=9$ has a lower limit of 400 gammas [51].

In the next chapter, the research methodology used for this study and how it has guided data collection, analysis technique and development of theory will be provided. The software used to collect the data, including formula implemented to maintain validity and reliability of the software are described.

CHAPTER 3

METHODOLOGY

3.1 Introduction

In order to ensure the scope of work to be done perfectly, many approaches were taken. This chapter was concentrated on the procedures in order to carry out research, which was briefly explained. So, the steps were taken properly and requirements of each step were fulfilled in order to complete the research successfully.

The first step is to identify the needs and requirement of the project. Before that, to have knowledge on the background of the problem statement of this project, the theoretical analysis on the variations of the ionosphere over the equatorial region and its effect to GPS positioning was carried out first. This is done by reviewing and understands previous related research works from relevant books and highly cited research papers.

The project planning in the format of project flowchart has been prepared to make sure the research can be conducted systematically according to the flow chart. Figure 3.1 shows a framework for overall project in this research.

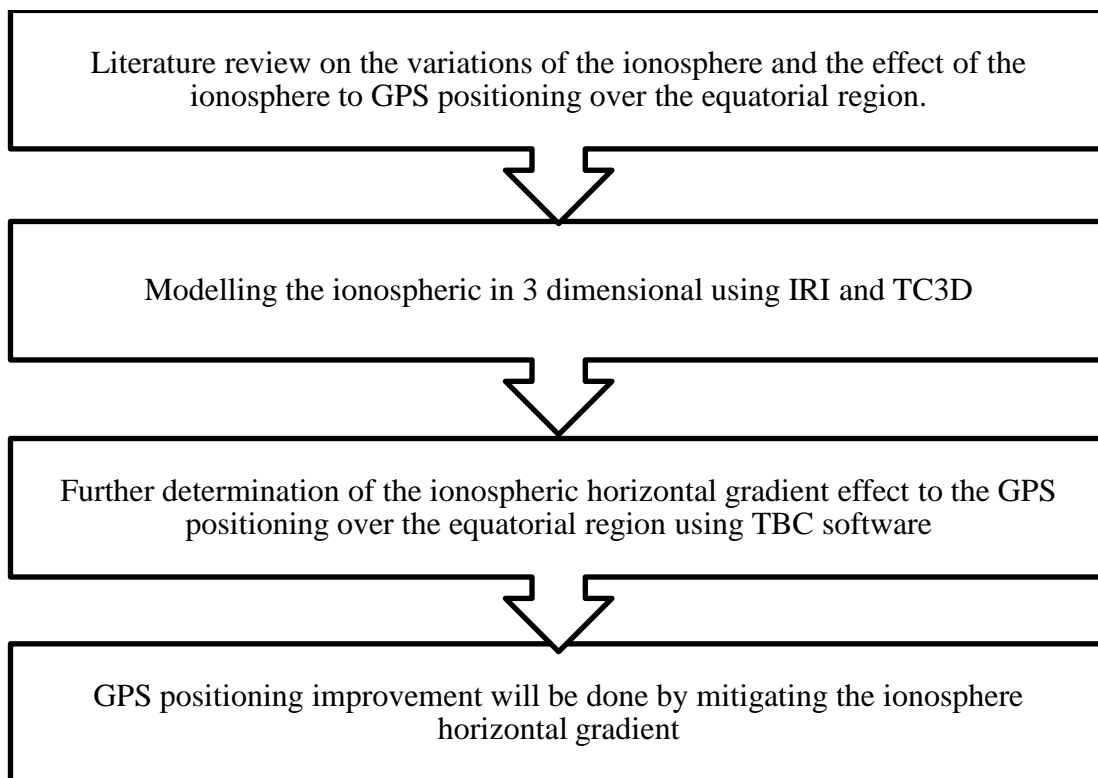


Figure 3.1: Flow chart for overall project

To conduct this research, there are few methods that need to be carried out. In brief, the methodology of this project can be simplified below;

- i. Study of the ionospheric error to GPS positioning over the equatorial region
Latest information of this subject area has been gathered and reviewed. This is useful to know the current establishments that have been done in this research area.

- ii. Modeling the ionosphere in 3 dimensional
The ionosphere has been modeled in latitude, longitude and electron density, N_e (3 dimensions) over the equatorial region (e.g. Malaysia). Existing ionosphere predictor such as IRI has been used to obtain the data. Software named TC3D can be used to do the 3D modeling. It helps to obtain the best analytical mathematical model that fits very well the variations of the ionosphere in 3 dimensions.

- iii. Trimble Business Centre (TBC) Software
The results obtained can be improved further by determining the ionospheric horizontal gradient effect to GPS positioning over the equatorial region. Improvement made by mitigating the ionospheric error.

Basically the work is divided into two parts; material or types of data and software that has been used in this research and the method or analysis techniques in order to perform the research. The detail about this work was discussed in the following section.

3.2 International Reference Ionosphere (IRI)

The International Reference Ionosphere or known very well as IRI is an international project sponsored by the Committee on Space Research (COSPAR) and the International Union of Radio Science (URSI) [12]. IRI is updated yearly. For a given location, time and date, IRI describes the N_e , electron temperature, ion temperature, and ion composition in the altitude range from about 50 km to about 2000 km, and also the electron content can define the variations of the N_e from bottom of the ionosphere to the altitude of maximum density. IRI is more accurate in describing the variations of the electron density from bottom of the ionosphere to the altitude of maximum density than in describing the TEC [12]. The performances of the IRI models in predicting the characteristics of the ionosphere using GPS have been investigated in [52] and shows that TEC reproduced by IRI and models are in good agreement with observed TEC. On the other hand, TEC calculation from IRI-2012 is better than IRI-2007 [52].

For this project, the data was collected from about one hour after sunrise to one hour before midnight at four different local times (LT) at 8.00am, 1.00pm, 6.00pm and 11.00pm from 1st June 2009 to 7th June 2009 to observe the diurnal electron density variation over the equatorial region during low solar activity. The N_e was obtained at 350 km altitude. This altitude was chosen to do this modelling as this has been presumed as the altitude where the content of the N_e is highest at this altitude [29]. Figure 3.2 show the part of the cross section of IRI-2012.

Virtual Ionosphere, Thermosphere, Mesosphere Observatory (VITMO)

International Reference Ionosphere - IRI-2012

This page enables the computation and plotting of IRI parameters: electron and ion (O^+ , H^+ , He^+ , O_2^+ , NO^+) densities, total electron content, electron, ion and neutral (NRL-MSIS-2002) temperatures, equatorial vertical ion drift and others.

[Go to the IRI description](#)

❖ **Select Date and Time**

Year(1958-2019):

Note: If date is outside the Ap index range (1958-2016 02/15), then STORM model will be turned off.

Month: Day(1-31):

Time: Hour of day (e.g. 1.5):

❖ **Select Coordinates**

Coordinates Type:

Latitude(deg. from -90. to 90.): Longitude(deg. from 0. to 360.):

Height (km. from 60. to 2000.):

❖ **Select a Profile type and its parameters:**

Height.km [60. - 2000.] Stepsize:

Figure 3.2: Part of the cross section of IRI-2012 [53]

3.3 Table Curve 3D (TC3D)

After data was collected, formation of mathematical model in three dimensions has been built. In this task, comprising TC3D has been used to form latitude, longitude and N_e in order to represent the ionosphere. TC3D gives scientists and engineers the knowledge to find the ideal model for even the most complex 3 dimensional data, including the equations that might never have been considered before [54].

The Figure 3.3 show that the process of fitting the database to create an equation with 3 dimension layout. For this project, assume the input data are X , Y and Z and they represent the values of longitude, latitude and N_e respectively. All these data was obtained from IRI 2012. By using an excel document, these values can be imported into the T3CD software to do the fitting. The values of X and Y would be specified in radians as it would be easier to use them later in Matlab to calculate the value of Z from the equation. The N_e from IRI has been compared with TC3D and from Matlab.

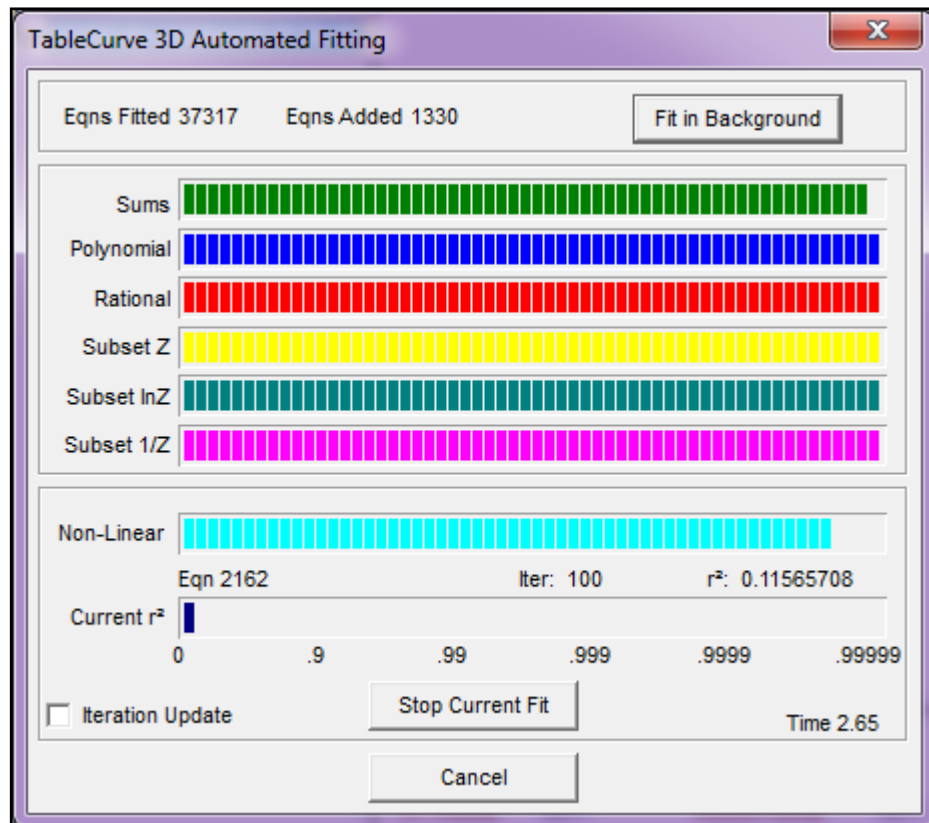


Figure 3.3: Table Curve 3D automated fitting process

To smooth the mesh plot or to get better fitting, the 'Options' can be adjusted so that the value of r^2 (coefficient of determination) will approach 1 (100%) and the SSE (Sum of Squared Errors) will approach 0. Approaching these figures will signify the best fitting. Then, the smoothed plot will be added to the main window. Once this has been done, TC3D will determine an equation that can best represent the given input data. Normally, the software will suggest the best equation (the equation with first rank) as in Figure 3.4. In this project, the form of an equation that can consist of only sine and cosine terms or their combinations was used to model the electron density. The sine and cosine functions are primarily chosen because (i.e. the exponential) their derivatives are always continuous, which is useful when the model being used in ray tracing program [9].

Eq#	Rank	r ²	FP	Eq#	Eqn
1	0.9997711388	315	539	Cosine Series Bivariate Order 10	
2	0.99969367	277	524	Fourier Series Bivariate Order 2x5	
3	0.999440169	270	538	Cosine Series Bivariate Order 9	
4	0.99893411	198	523	Fourier Series Bivariate Order 2x4	
5	0.9988828604	228	537	Cosine Series Bivariate Order 8	
6	0.9987997481	334	510	Fourier Series Simple Order 2x10	
7	0.9987994373	300	509	Fourier Series Simple Order 2x9	
8	0.9987989222	267	508	Fourier Series Simple Order 2x8	
9	0.998798105	234	507	Fourier Series Simple Order 2x7	
10	0.9987719272	200	506	Fourier Series Simple Order 2x6	
11	0.9985526194	167	505	Fourier Series Simple Order 2x5	
12	0.997934977	134	504	Fourier Series Simple Order 2x4	
13	0.9977391199	190	536	Cosine Series Bivariate Order 7	
14	0.9974347123	154	535	Cosine Series Bivariate Order 6	
15	0.9960779342	122	534	Cosine Series Bivariate Order 5	
16	0.9934910257	131	522	Fourier Series Bivariate Order 2x3	
17	0.992886598	100	503	Fourier Series Simple Order 2x3	
18	0.9913031115	20	65	$Z=a+bx+cx^2+dx^3+ex^4+fx^5+gy+hy^2+iy^3+jy^4+ky^5$	
19	0.9913031113	21	75	$Z=a+bx+cx^2+dx^3+ex^4+fx^5+g/y+h/y^2+i/y^3+j/y^4+ky^5$	
20	0.9913031101	18	64	$Z=a+bx+cx^2+dx^3+ex^4+fx^5+gy+hy^2+iy^3+jy^4$	
21	0.9913031098	25	70	$Z=a+bx+cx^2+dx^3+ex^4+fx^5+g\ln y+h(\ln y)^2+i(\ln y)^3+j(\ln y)^4+k(\ln y)^5$	
22	0.9913031095	19	74	$Z=a+bx+cx^2+dx^3+ex^4+fx^5+g/y+h/y^2+i/y^3+j/y^4$	
23	0.991303109	16	63	$Z=a+bx+cx^2+dx^3+ex^4+fx^5+gy+hy^2+iy^3$	
24	0.9913031089	23	69	$Z=a+bx+cx^2+dx^3+ex^4+fx^5+g\ln y+h(\ln y)^2+i(\ln y)^3+j(\ln y)^4$	
25	0.9913031087	17	73	$Z=a+bx+cx^2+dx^3+ex^4+fx^5+g/y+h/y^2+i/y^3$	
26	0.9913031081	21	68	$Z=a+bx+cx^2+dx^3+ex^4+fx^5+g\ln y+h(\ln y)^2+i(\ln y)^3$	
27	0.9913031062	19	67	$Z=a+bx+cx^2+dx^3+ex^4+fx^5+g\ln y+h(\ln y)^2$	

Figure 3.4: The equation list after surface fit all equations

At the same time, TC3D also produced Data Summary and Numeric Summary files (Appendix A-B). The Data Summary file will show the data values that have been input through the Excel file (X , Y and Z values). Then TC3D will use the given X , Y and Z values to 'calculate' another set of Z values; called the predicted Z values. These predicted Z values together with the X and Y values will be used to find an equation. The differences between the true Z values and the predicted Z values are shown as residuals which can also be obtained from the Data Summary file. The Numeric Summary file will give the values of parameters that are used in the equation. Basically, both files are required if the values of Z will be calculated using Matlab. Both files can be saved in the *.txt format and then can be used later to do the calculations. Therefore, this software has been used to get an equation or model of N_e , which varies over a specific region of longitude and latitude at one specific height. The process of modelling the diurnal variation of ionosphere was done by using TC3D whereby the data was obtained from the IRI as shown in Figure

REFERENCES

1. A. Gebremedihh. *Tomographic Imaging Of Ionospheric Electron Density Over Eastern Africa Using Multi-Platform Instrumentations And Model Ionospheric Total Electron Content*. Ph.D. Thesis. Addis Ababa University, Ethiopia. 2013.
2. P. Misra and P. Enge. *Global Positioning System: Signals, Measurements, and Performance*. 2nd ed. Ganga-Jamuna Press. 2011.
3. O. Ørpen. Solar Activity and the Effect on Positioning Systems - The first Examples of Disturbances in Solar Cycle 24. *European Navigation Conference*. London. 2013. pp. 6–11.
4. V. S. Srinivas, A. D. Sarma, A. Supraja Reddy, and D. Krishna Reddy. Investigation of the effect of ionospheric gradients on GPS signals in the context of LAAS. *Progress Electromagnetic Research B*. 2014. vol. 57(57): pp. 191–205.
5. C. S. Fah. Significant of Earth's Magnetic Field and Ionospheric Horizontal Gradient to GPS Signals. *Proceeding of the 2013 IEEE International Conference on Space Science and Communication (IconSpace)*. 2013. no. July. pp. 1–3.
6. K. Nagarajoo. DGPS Positioning Improvement by Utilizing the Ionospheric Horizontal Gradient Factor. *Malaysia Annual Physics Conference*. 2011. vol. 164: pp. 2011–2014.
7. K. Nagarajoo. DGPS positional improvement by mitigating the ionospheric horizontal gradient using GPSurvey. *2011 IEEE International Conference on Space Science and Communication: Towards Exploring the Equatorial Phenomena (IconSpace 2011) - Proceedings*. 2011. pp. 65–68.
8. K. Nagarajoo. DGPS Positional Improvement by Mitigating the Ionospheric Horizontal Gradient and Elevation Angle Effects. *Proceedings of 2010 IEEE*

- Asia-Pacific Conference on Applied Electromagnetics (APACE 2010)*. 2010. no. 0660.
9. K. Nagarajoo. *Improved Ionospheric Correction for Dual Frequency and Differential GPS Positioning Methods*. Ph.D. Thesis. The University of Leeds. 2007.
 10. N. Ya'acob, M. Abdullah, and M. Ismail. Ionospheric Modelling : Improving The Accuracy of Differential GPS (dGPS) in Equatorial Regions. *2007 Asia-Pacific Conference on Applied Electromagnetics Proceedings (APACE2007)*. 2007. pp. 0–4.
 11. U. Dogan, M. Uludag, and D. O. Demir. *Investigation of GPS positioning accuracy during the seasonal variation*. Elsevier. 2014. vol. 53: pp. 91–100.
 12. D. Bilitza (2012). *International Reference Ionosphere (IRI-2007)*. National Aeronautics and Space Administration (NASA). Retrived on April 22, 2012, from <http://ccmc.gsfc.nasa.gov/modelweb/ionos/iri.html>.
 13. Z. M. Artinian. *The Atmosphere*. Bridges Ed. Benchmark Education Company. 2010. pp. 15.
 14. Stefan. F. Bush. *Smart Grid: Communication-Enabled Intelligence for the Electric Power Grid*. John Wiley & Sons. 2014.
 15. Leo F. McNamara. *Radio Amateurs Guide to the Ionosphere*. USA: Krieger Pub Company. 1994.
 16. P. K. Subhadra Devi. *Behaviour of ionosphere and its interaction with solar magnetosphere system*. Master Thesis. Mahatma Gandhi University. 2014.
 17. National Aeronautics and Space Administration (NASA) (2013). *Earth's Atmospheric Layers*. Retrived on August 20, 2013, from http://www.nasa.gov/images/content/463940main_atmosphere_layers2_full.jpg.
 18. U.S. Department of Defense. *Communications-Electronics Fundamentals: Wave Propagation, Transmission Lines, and Antennas*. United States: Department of the Army. 2014.
 19. Walter Dieminger, Gerd K. Hartmann, Reinhart Leitinger. *The Upper Atmosphere: Data Analysis and Interpretation*. Springer Science & Business Media. 2011.

20. I. Poole (2012). *The Ionosphere and Radiowave Propagation*_Radio-Electronics.com. Retrived on June 06, 2014, from <http://www.radio-electronics.com/info/propagation/ionospheric/ionosphere.php>.
21. J. Asgari and A. R. Amiri-Simkooei. Analysis and Prediction of GNSS Estimated Total Electron Contents. *Journal of the Earth & Space Physic*. 2011. vol. 37(1): pp. 11–24.
22. M. M. Amin. *Influence of lightning on electron density variation in the ionosphere using WWLLN lightning data and GPS data*. Ph.D. Thesis. Department of Electrical Engineering, University of Cape Town. 2015.
23. J. A. Klobuchar. *Global Positioning System: Theory and Applications*. American Institute of Aeronautics and Astronautics. pp. 485–516. 1996
24. N. Ya’acob, M. Abdullah, and M. Ismail. *GPS Total Electron Content (TEC) Prediction at Ionosphere Layer over the Equatorial Region*. Trends in Telecommunications Technologies. 2000. pp. 485–508.
25. W. Y. Ng, S. A. Bahari, M. Abdullah, and B. Yatim. Regional Ionosphere Maps over Malaysia during Solar Minimum. *Proceeding of the 2009 International Conference on Space Science and Communication*. October 2009. Port Dickson, Negeri Sembilan. pp. 161–165.
26. R. S. Fayose, R. Babatunde, O. Oladosu, and K. Groves. Variation of Total Electron Content (TEC) and Their Effect on GNSS over Akure, Nigeria. 2012. *Applied Physics Research*. vol. 4 (2): pp. 105–109.
27. C. Carter. *Principles of GPS Positioning: A Brief Primer on the Operation of the Global Positioning System*. CSR Technology, Inc. 2012.
28. D. Wyatt and M. Tooley. *Aircraft Communications and Navigation Systems*. Routledge. 2013.
29. G. S. Rao. *Global Navigation Satellite Systems*. Tata McGraw-Hill Education. 2010.
30. G. R. Dharani and N. B. Sabares. AEGPS (Accuracy Enhanced Global Positioning System) - Based on case study. *2012 International Conference on Information and Network Technology (ICINT 2012)*. 2012. vol. 37. pp. 183–187.
31. H. Peter Dana (Department of Geography, University of Colorado Boulder) (2004). *Global Positioning System Overview*. Retrived on September 26, 2014, from http://www.colorado.edu/geography/gcraft/notes/gps/gps_f.html.

32. T. J. Jyrki, Penttinen. *The Telecommunications Handbook: Engineering Guidelines for Fixed, Mobile and Satellite Systems*. USA: John Wiley & Sons. 2015.
33. W. Xinlong and L. Yafeng. Study on adaptability of GPS ionospheric error correction models. 2009. *Aircraft Engineering and Aerospace Technology*. vol. 81(4): pp. 316 – 322.
34. M. S. Grewal, L. R. Weill, and A. P. Andrews. *Global Positioning Systems, Inertial Navigation, and Integration*. 2nd ed. New Jersey: John Wiley & Sons. 2007.
35. *Trimble-GPS Tutorial: How does Differential GPS works*. Retrived on January 23, 2013, from http://www.trimble.com/gps_tutorial/dgps-how.aspx.
36. T. Matsushita, T. Tanaka, and M. Yonekawa. Improvement of Measurement Accuracy with Long Baseline Reference Stations in DGPS. *Journal of the Institute of Positioning, Navigation and Timing of Japan*. 2011. vol. 1(1): pp. 1–8.
37. M. Chivers (2013). *Differential GPS Explained*. Retrived on February 21, 2015, from <http://www.esri.com/news/arcuser/0103/differential1of2.html>
38. K. Nagarajoo. Variable methods to estimate the ionospheric horizontal gradient. *8th IGRSM International Conference and Exhibition on Remote Sensing & GIS (IGRSM 2016)*. 2016. IOP Publishing. vol. 37: pp. 012012.
39. K. Nagarajoo. Correction of the Ionospheric Horizontal Gradient for Better DGPS User Positioning. *International Journal of Engineering and Innovative Technology (IJEIT)*. 2013. vol. 2(7): pp. 413–416.
40. J. Spencer, B. G. Frizzelle, P. H. Page, and J. B. Vogler. *Global Positioning System: A Field Guide for the Social Sciences*. John Wiley & Sons. 2008.
41. R. B. Langley. *Dilution of Precision*. *GPS World*. vol. 10(May): pp. 52–59. 1999.
42. R. Tiwari, S. Bhattacharya, P. K. Purohit, and A. K. Gwal. Effect of TEC Variation on GPS Precise Point at Low Latitude. *The Open Atmospheric Science Journal*. 2009. vol 3: pp. 1–12.
43. M. Richharia and L. D. Westbrook. *Satellite Systems for Personal Applications: Concepts and Technology Volume 22 of Wireless Communications and Mobile Computing*. John Wiley & Sons. 2011.

44. J. Frédéric Pont. *Alien Skies: Planetary Atmospheres from Earth to Exoplanets*. Springer. 2014.
45. Marshall Space Flight Center National Aeronautics and Space Administration (NASA) (2015). *Cycle 24 Sunspot Number Predictions*. Retrived on November 23, 2015, from <http://solarscience.msfc.nasa.gov/images/Cycle22Cycle23Cycle24big.gif>.
46. C. J. Schrijver, W. C. Livingston, T. N. Woods, and R. A. Mewaldt. The minimal solar activity in 2008-2009 and its implications for long-term climate modeling. *Geophysical Research Letters*. vol. 38(6): pp. 1–6, 2011.
47. The Old Farmer's Almanac (2013). *Solar Activity, Solar Cycle Predictions, and Sunspots*. Retrived on July 23, 2012, from <http://www.almanac.com/sunspotupdate>.
48. NASA Marshall Space Flight Center Solar Physic Group (2014). *Sunspot Cycle*. Retrived on September 15, 2014, from <http://solarscience.msfc.nasa.gov/SunspotCycle.shtml>.
49. O. F. Nneka, O. S. Ebere, and H. E. Akpan. Investigation of electron density variation in some regions of the Ionosphere at Nsukka, Nigeria. 2009. *International Journal of Library and Information Science*. vol. 1(2): pp. 12–16.
50. NOAA National Geophysical Data Center (2014). *Geomagnetic kp and ap Indices*. Retrived on October 19, 2014, from http://www.ngdc.noaa.gov/stp/geomag/kp_ap.html.
51. NOAA National Geophysical Data Center (2014). *Selected Geomagnetic And Solar Activity Indices*. Retrived on October 19, 2014, from ftp://ftp.ngdc.noaa.gov/STP/GEOMAGNETIC_DATA/INDICES/KP_AP/kp_ap.fmt.
52. S. K. Leong, T. A. Musa, K. Omar, M. D. Subari, N. B. Pathy, and M. F. Asillam. Assessment of ionosphere models at Banting: Performance of IRI-2007, IRI-2012 and NeQuick 2 models during the ascending phase of Solar Cycle 24. *Advances in Space Research*. 2015. vol. 55(8), pp. 1928–1940.
53. International Reference Ionosphere - IRI-2012. (2016). Retrived on March 19, 2016, from http://omniweb.gsfc.nasa.gov/vitmo/iri2012_vitmo.html.
54. *TableCurve3D: Automated Surface Fitting Analysis* (2016). Retrived on March 19, 2016, from

http://www.sigmaplot.com/products/tablecurve3d/tablecurve3d_4_brochure.pdf

55. Trimble Business Center. Version 2.70. *Release Notes*. Ohio. 2012.
56. Y. B. Yao, P. Chen, S. Zhang and J. J. Chen. Temporal and spatial variations in ionospheric electron density profiles over South Africa during strong magnetic storms. *Natural Hazards and Earth System Science*. 2013. vol. 13(2): pp. 375–384.
57. X. Zhang, X. Shen, J. Liu, Z. Zeren, L. Yao, X. Ouyang, S. Zhao, G. Yuan, and J. Qian. The solar cycle variation of plasma parameters in equatorial and mid latitudinal areas during 2005-2010. *Advances in Space Research*. 2014. vol. 54(3): pp. 306–319.
58. F. Ouattara, D. A. Gnabahou, and C. A. Mazaudier. Seasonal, Diurnal and Solar-Cycle Variations of Electron Density at Two West Africa Equatorial Ionization Anomaly Stations. *International Journal of Geophysics*. 2012. vol. 2012: pp. 9.
59. E. Mohíno Harris, M. Gende, and C. Brunini. A Method for Ionospheric Bias Mitigation in Differential GPS Positioning Using Multiple Reference Stations. *Journal of Surveying Engineering*. 2010. vol. 133(1): pp. 1–5.
60. C. Okorochoa and O. Olajugba. Comparative Analysis of Short, Medium and Long Baseline Processing in the Precision of GNSS Positioning. *FIG Congress 2014 Engaging the Challenges - Enhancing the Relevance*. June 2014. pp. 7005.
61. S. K. Panda, S. S. Gedam and G. Rajaram. Ionospheric Characteristics of Low Latitude Anomaly Zone Over Indian Region by Ground Based GPS, Radio Occultation and SPIM Model Predictions. *IGARSS 2013*. pp. 1839–1842.